A Model for the Electrical Resistivity of 2-Phase Anisotropic Geological Materials

Michelle H. Ellis[*,1], Martin C. Sinha[1], Tim A. Minshull[1], Jeremy Sothcott[1], and Angus I. Best[1].

[1]Geology and Geophysics Research Group, National Oceanography Centre Southampton, University of Southampton Waterfront Campus, European Way, Southampton, SO14 3ZH, U.K.

[*]Corresponding author: Michelle Ellis, e-mail: mhe1@noc.soton.ac.uk

Submitted to Geophysics:

Accepted:

ABSTRACT

We present a physical model for estimating the bulk electrical resistivity of clastic sediments. The approach makes use of the increase in path length taken by an electrical current through an idealized sediment consisting of ellipsoidal grains. This method has advantages over the traditional Archie's method because is it able to predict the effects of grain aspect ratio and anisotropy. The method also permits both the solid and fluid phases some conductivity. The model is grain size independent, allowing it to be applied to a wide range of sediment types. The method is validated through comparison with laboratory resistivity measurements made on artificial sediment samples with known physical properties.

INTRODUCTION

Measurements of electrical resistivity are commonly used in petroleum exploration to investigate the nature of sedimentary formations and especially the water saturation in hydrocarbon reservoirs. Geophysical techniques that use electrical resistivity include borehole induction logging a well-established method, and seafloor Controlled Source Electro-Magnetic (CSEM) surveying which is emerging as a powerful hydrocarbon exploration tool. The interpretation of such resistivity measurements relies on knowledge of the relationships between the effective (bulk) resistivity and the physical properties of the constituent parts of the sediment (i.e., solid minerals and interstitial fluid). The electrical resistivity of a sediment is primarily controlled by porosity, pore fluid saturation, pore fluid salinity, temperature, mineralogy (quartz, feldspar, clay, carbonate, etc.), and grain fabric (e.g., grain shape and alignment).

The standard method of interpreting electrical resistivity data for sedimentary sequences, especially in well log interpretation, involves the use of Archie's (1942) equation. Archie (1942) showed experimentally that the resistivity of clean sandstone is proportional to the resistivity of the brine saturating the sandstone. The proportionality constant is known as the formation factor (F) and can be related to the porosity of saturated sandstone using an empirical relationship:

$$F = \frac{\rho_o}{\rho_f} = a\varphi^{-m}, \tag{1}$$

where ρ_f and ρ_o are the resistivities of the fluid and the fully saturated sedimentary medium respectively and m and a are empirical constants. The constant a represents

the ‘tortuosity factor’ of the system, m is the ‘cementation exponent’, and φ is the porosity. The advantage of this approach is that it is simple. The empirical constants within the equation can be varied such that it can fit almost any data set. Formation factor versus porosity curves can be determined for different lithologies and these are used extensively in the hydrocarbon industry (Schlumberger, 1977). Archie’s equation is however purely empirical and so the cementation and tortuosity constants cannot be physically justified. In addition a large data set is usually needed to determine these constants, although approximate values have been determined for several different types of sediments (Schlumberger, 1977).

Using a physical model to estimate resistivity is more desirable for several reasons. Firstly, empirical constants must be derived from an initial data set. The initial data may not span the entire porosity range, and the empirical constants calculated from the initial data cannot always be used outside the original data range (Berg, 1995), leading to errors. Secondly, the empirical constants that are determined for one data set cannot necessarily be applied to another data set. Thirdly, because the constants can be freely varied, they can be forced to fit almost any data set, which may lead to incorrect interpretation. Using a physical model is also desirable because the model can be made physically compatible with one or more of the seismic effective medium models which are in widespread use. Physically consistent electrical and seismic effective medium models would be useful for jointly interpreting combined geophysical datasets, and would lead to a more complete understanding of the nature of the sediment being investigated.

There are very few numerical effective medium models for resistivity that are purely physical, and contain no empirical constants. In order to predict the effective resistivity of a multi-component medium, three requirements need to be specified (Mavko et al., 2003): (1) the volume fraction of each of the components; (2) the electrical resistivity of each of the components; and (3) the geometrical relationship between the components. The most widely used purely physical models are the Hashin-Shtrikman (HS) conductivity bounds (Hashin and Shtrikman 1962) and the Hanai-Bruggeman (HB) equation (Hanai, 1960; Bruggeman, 1935). One of the main advantages that both of these models have over Archie's equation is that they allow the solid phase to have a finite conductivity. This is particularly important when estimating the electrical resistivity of sediments containing clay minerals. Clay minerals can conduct charge through electric double layers and have large surface area to volume ratios, causing them to contribute significantly to the effective conductivity (reciprocal of resistivity) of the sediment. Resistivity models for clays developed by Wyllie and Southwick (1954), Waxman and Smits (1968), Clavier (1984), Bussian (1983), and Berg (1995) all suffer from the same limitation as Archie's equation, namely they all require at least one empirically derived constant to account for the grain's geometrical arrangement. Several of the models require multiple empirical constants.

One of the main disadvantages of the HS method is that the geometrical relationship between the matrix and the pore fluids is not taken into account, and as a result only upper and lower bounds of resistivity can be determined. Also since the geometry between the different phases is not specified, the models must assume that the effective medium is isotropic. The HB equation uses a Differential Effective

Medium (DEM) approach to determine the effective resistivity of a medium which contains spherical inclusions. Unlike the HS bounds it does specify a geometric relationship between the phases. However, there are several problems with the HB bound. Firstly it assumes that the solid phase is totally interconnected while the fluid phase inclusions are isolated, which is unrealistic in nature. However, Sen et al. (1981) used a similar DEM method which reverses the solid and fluid phases to overcome this problem. Secondly, only spherical inclusions are used within the model, which again is not always realistic when representing a sediment. Thirdly, as a consequence of the spherical inclusions, the model requires that the final effective medium is isotropic. Anisotropy can be caused by the alignment of sediment grains with aspect ratios less than one. This alignment often occurs in shales and mudstones, leading to large degrees of electrical anisotropy (Anderson and Helbig, 1994; Clavaud 2008). It is therefore important to develop a method in which grain shape and grain alignment can also be taken into account, so that anisotropic media can be modeled.

In this paper we present an electrical effective medium model which is based on the physical arrangement of the phases, in which the fluid is interconnected, and in which we specify the shape and alignment of the grains. The physical parameterization of the medium is identical to that used in a number of widely applied seismic effective medium models. In the second part of the paper we validate our model by comparing its predictions to laboratory measurements made on artificial sediments.

ELECTRICAL EFFECTIVE MEDIUM MODEL

The presence of relatively resistive grains in a conductive fluid influences the effective resistivity in several ways:

(1) The grains reduce the cross-sectional area of conduction through which the electric current must flow. This also means that the current density through the more conductive phase is increased, while the current density through the proportion of the original volume now occupied by the more resistive phase is decreased.

(2) Since in general the current is no longer directly aligned with the ambient electric field, there is an increase in the 'path-length' as the current will preferentially travel around the grains rather than through them.

(3) The grain density influences the proportion of the path length which is deviated in order to travel around the grains, and the proportion of the path length which is not deviated.

This section develops an electrical effective medium model which takes into account all three of these factors but which remains purely physically based (i.e., requiring no empirical constants).

Hashin-Shtrikman bounds

The first factor can be accounted for by using the Hashin-Shtrikman (HS) resistivity bounds (Hashin and Shtrikman, 1962) as the starting point for our model. The HS bounds give the narrowest possible isotropic bounds without defining the geometry between components of a two-phase medium. All the components within this medium are themselves isotropic and homogeneous. The upper bound represents the maximum conductivity the isotropic composite can have. This occurs when the fluid (conductive phase) is totally interconnected and the solid (resistive phase) occurs

as totally isolated inclusions. The HS lower or resistive bound represents the bound when the fluid phase occurs as completely isolated inclusions, and the solid phase is totally interconnected. No other information is given about the geometry system. The HS bounds are given by:

$$\frac{1}{\rho_{HS,conductive}} = \sigma_{HS,conductive} = \sigma_f + (1-\beta)\left(\frac{1}{\sigma_s - \sigma_f} + \frac{\beta}{3\sigma_f}\right)^{-1}, \quad (2)$$

$$\frac{1}{\rho_{HS,resistive}} = \sigma_{HS,resistive} = \sigma_s + \beta\left(\frac{1}{\sigma_f - \sigma_s} + \frac{1-\beta}{3\sigma_s}\right)^{-1}, \quad (3)$$

where $\sigma_{HS,conductive}$ is the upper or conductive HS bound of effective conductivity, $\sigma_{HS,resistive}$ is the lower or resistive HS bound of effective conductivity, $\rho_{HS,conductive}$ and $\rho_{HS,resistive}$ are the conductive and resistive HS bounds of the effective resistivity respectively. σ_s and σ_f are the conductivities of the solid and fluid respectively and β is the volumetric fraction of the fluid (assumed to be equal to the porosity). The physical relationship between the pore fluids and the solid grains in an uncemented clastic sediment is represented best by the HS conductive bound (rather than the resistive bound) where all the fluid is interconnected. Therefore we use the conductive bound as the starting point for our model.

Geometric factor

The second factor can be addressed by investigating the influence of the average increase in path length that the electric current has to take to pass through the sediment. This can be represented as a geometric factor. Herrick and Kennedy (1994) used the path a current takes through a formation to determine the effective resistivity. Their model assumes that the formation can be represented as a solid volume (representing the matrix) with a series of tubes running through it representing the

pores. A geometrical parameter can be calculated from the size, shape and number of tubes and then used to determine the effective resistivity of the formation. The problem with this method is that it cannot represent completely the complex pore geometry observed in sediments. Rather than trying to model the complex shapes of pores, the geometric factor developed in this paper concentrates on estimating the change in current path caused by the grains. In practice, the electric current will typically take the form of mobile ionic charge carriers (anions and cations) dissolved in the pore fluid. The charge carriers, and so electric current, will take the shortest available route through the sediment along the direction of the imposed electric field; but this is longer than the actual length of sediment because the current must go around the grains (Figure 1).

In order to calculate the increase in path length, the grains of a sediment are idealized. A sphere - an ellipsoid with an aspect ratio of one - is the simplest shape and can be used to model a sand grain. Taking a simple example, suppose that a charge carrier encounters a spherical grain at its centre. The charge carrier will be deviated at most around half of the circumference of the grain, and leave it at its opposite 'pole' (Figure 1). If the diameter of the sphere is d, then the undeviated path length l_1 would also be d; however the deviated path length l_2 is half the circumference, $\pi d/2$. The geometric factor, l_1/l_2, is then given by $\frac{\pi d}{2d} = \frac{\pi}{2}$ or approximately 1.57. Assuming therefore that the increase in path length is due to a spherically shaped grain, the increase can be up to 57%, causing the resistivity of the medium to increase by the same amount. $\mp \int$

This value assumes that the electric current encounters the sphere at its centre and then travels around the grain to the opposite pole, at which point the current continues along its original path. However the current (charge carrier) may encounter the grain at any point on the grain surface which is in the path of the current; therefore the average increase in path length for randomly distributed charge carriers needs to be calculated. It is assumed that when the current encounters the grain it will travel around the grain until it reaches a point at which it can continue in the fluid along its original path. This requirement forces the current to redistribute itself as it passes around the grain, and imposes a condition on the model that once clear of the grain, the electric current density within the fluid phase becomes uniform and aligned along the direction of the imposed electric field, until another grain is encountered. Using this simple model we can assume that (1) a current path that does not directly encounter a grain will suffer no deviation. (2) a current path that encounters a grain is deviated around its circumference until it reaches the corresponding point on the other side.

To calculate the geometric factor, i.e., the fractional increase in path length, both the deviated path length (l_1) and the undeviated path length (l_2) need to be calculated (Figure 2).

In this case:

$$l_1 = 2\left[\frac{\pi r}{2} - r\gamma\right] = 2\left[\frac{\pi r}{2} - r\sin^{-1}\left(\frac{w}{r}\right)\right], \tag{4}$$

$$l_2 = 2\left(r^2 - w^2\right)^{1/2}, \tag{5}$$

where:

$$w = r\sin\gamma\,. \tag{6}$$

The geometrical factor (g) can then be calculated as follows:

$$g = {l_1}/{l_2} = \frac{\frac{\pi r}{2} - r\gamma}{\sqrt{r^2 - (r\sin\gamma)^2}} = \frac{\frac{\pi}{2} - \gamma}{\sqrt{\cos(\gamma)}}, \tag{7}$$

Because both l_1 and l_2 are proportional to the radius, the rs cancel out. The geometric factor is therefore independent of the size of the grain. This is an important result for the practical application of any effective medium model.

When viewed from above the grain appears as a circle, on which the current may hit at any point (Figure 2). To obtain the average geometric factor (G) the ratio must be calculated at every point over the grain's cross-section.

$$G = {l_{1ave}}/{l_{2ave}} = \frac{\int_{x=0}^{r}\int_{y=0}^{\sqrt{r^2-x^2}} l_1 .dydx}{\int_{x=0}^{r}\int_{y=0}^{\sqrt{r^2-x^2}} l_2 .dydx}, \tag{8}$$

where:

$$w = \left(x^2 + y^2\right)^{1/2}. \tag{9}$$

x and y are the corresponding coordinates of the point where the current encounters the grain, with the origin taken at the grain centre. l_{1ave} and l_{2ave} are the average l_1 and l_2 values over the entire sphere. Evaluating this double integral numerically, we determine that for a sphere the geometric factor is 1.178 (4 s.f.).

The resistivity of the fluid is multiplied by the geometric factor to give a new, higher, fluid effective resistivity which accounts for the extra distance traveled by the

electrical current. This new fluid effective resistivity is then used with the HS conductive bound to give a new geometric effective resistivity of the medium (ρ_{geo}):

$$\frac{1}{\rho_{geo}} = \sigma_{geo} = \frac{\sigma_f}{G} + (1-\beta)\left(\frac{1}{\sigma_s - \frac{\sigma_f}{G}} + \frac{G\beta}{3\sigma_f}\right)^{-1} . \quad (10)$$

Mean path length

The geometric factor, as calculated above, cannot simply be applied to the HS conductive bound at all porosities because this will always have the effect of increasing the estimated resistivity. This would cause the estimated resistivity of the medium to be greater than the resistivity of the fluid at 100% porosity. Therefore a method is needed to determine the percentage of the fluid to which the geometric factor must be applied, so that at 100% porosity the geometric factor is not applied and thus address point 3.

The current will spend a certain proportion of the total path length being deviated around the grains, with the remainder of the path length being un-deviated (as it passes through the pores). The individual proportions will depend on the porosity of the sediment.

To calculate the average distance traveled by the current between the grains, an adapted version of the mean free path, which is used in the kinetic theory of gases to calculate the average distance between molecule collisions, can be used. The definition of the mean free path (L) is taken as the length (l) of a path divided by the number of collisions in that path and is given as:

$$L = \frac{1}{\sqrt{2} n_v S_c}, \quad (11)$$

where n_v is the number density of particles and S_c is the effective collision cross-section. The $\sqrt{2}$ term is included because in kinetics the molecules are considered to be moving. In our application all of the grains are stationary and therefore this term can be left out. In kinetics S_c is given by πd^2 where d is the diameter of the molecules. It is assumed that both the molecules involved in the collision have volume. In the case of an electric current encountering a grain, the electric current element (charge carrier) can be said to have infinitely small cross-section relative to the sediment grain, and the collision cross section will therefore be solely dependent on the cross-section of the grain. Therefore S_c will be given as πr^2.

The number density (n_v) is given by:

$$n_v = \frac{n_g}{\pi r^2 l}. \tag{12}$$

Where n_g is the number of grains and $\pi r^2 l$ is the volume that the grains occupy (r is the radius of the grains). The mean free path (L) is then given by:

$$L = \frac{1}{\pi r^2 \frac{n_g}{\pi r^2 l}} = \frac{l}{n_g}, \tag{13}$$

and for sediment with porosity β the number of grains (n_g) is given by:

$$n_g = \frac{\pi r^2 l(1-\beta)}{\frac{4}{3}\pi r^3} = \frac{l(1-\beta)}{\frac{4}{3}r}, \tag{14}$$

where $\pi r^2 l(1-\beta)$ is the volume of all the grains and $\frac{4}{3}\pi r^3$ is the volume of a single grain. Therefore for an imaginary electric current line passing through sediment with porosity β:

$$L = \frac{l}{\frac{l(1-\beta)}{\frac{4}{3}r}} = \frac{4r}{3(1-\beta)}. \tag{15}$$

In this equation L, the mean free path length, represents the mean distance between grain centers. L can then be used to determine the deviated and un-deviated proportions of the total path length though a composite medium. If we consider vertical current flow and grains of finite size then the geometric relationship between the average undeviated path length (l_{2ave}), grain radius (r), and the mean free path (L) can be seen in Figure 3.

Using equations 15 and 8 for L and l_{2ave} we can calculate the proportion of the total path length that is deviated by grains and the proportion that passes straight through the fluid (F_{grain} and F_{fluid} respectively):

$$F_{grain} = \frac{l_{2ave}}{L}, \tag{16}$$

$$F_{fluid} = 1 - F_{grain}. \tag{17}$$

Because both L and l_{2ave} are proportional to the radius of the grains, the deviated and undeviated proportions are again independent of the grain radius, and only dependent on the porosity. The resulting proportions of deviated and undeviated path length can now be used to navigate between the HS conductive bound (equation 2) and the geometrically altered HS conductive bound (ρ_{geo}, equation 10):

$$\frac{1}{\rho_{GPL}} = \left(\frac{1}{\rho_{HS,conductive}} F_{fluid} \right) + \left(\frac{1}{\rho_{geo}} F_{grain} \right) \tag{18}$$

where $\rho_{GPL\ GPL}$ is the geometric path length effective resistivity (Figure 4). It can be seen that at 100% porosity, ρ_{GPL} and $\rho_{HS,conductive}$ are the same. As the porosity decreases, ρ_{GPL} leaves the HS bound and moves towards ρ_{geo}.

Changing grain aspect ratio to simulate electrical anisotropy

Electrical anisotropy can be achieved using our geometric method by altering the aspect ratio of the grains. Instead of dealing with circles and spheres we are now dealing with ellipses and ellipsoids. However the problem remains tractable. An ellipse can be defined in Cartesian coordinates:

$$\frac{x^2}{a^2}+\frac{y^2}{b^2}=1. \tag{19}$$

The equation for an ellipsoid is:

$$\frac{x^2}{a^2}+\frac{y^2}{b^2}+\frac{z^2}{c^2}=1, \tag{20}$$

where *a, b* and *c are the* semi-axes of the ellipse and ellipsoid. The semi axes may have any length however in the following equations we shall consider the case where at least two of the axes have the same length.

Before the arc length can be determined, the shape of the grains needs to be defined. In this study we investigate two grain shapes: oblate and prolate. Once the shape is defined the orientation of the grains must be specified. In the following cases the grains will be oriented so that the electric current is traveling parallel to the c-axis (Figure 5). The arc length (*S*) for the ellipsoid can be given as:

$$S=\int_Q^P \sqrt{\left(\frac{dx}{dt}\right)^2+\left(\frac{dy}{dt}\right)^2+\left(\frac{dz}{dt}\right)^2}\,dt, \tag{21}$$

where *P* and *Q* are the end points of the arc and *t* is a parametric value. In the case of a current element (charge carrier) encountering the grain, *P* and *Q* are the points where the current starts and ceases to be deviated. As in the case of a sphere the mean path length must be determined by averaging the path length over the whole surface of the grain. Equation 18, which was used in the case of the spherical grain, can be used again to determine *G* for an ellipsoidal grain. In this case:

$$l_1 = S\,, \tag{22}$$

and

$$l_2 = 2z\,, \tag{23}$$

where z is given by equation 20.

Again we have integrated numerically the resulting expressions. For grains aligned in the least resistive direction (i.e., the current is traveling parallel to the long axis, Figure 5) there is relatively little variation between the prolate and the oblate grains (Figure 6). The largest change in the geometric factor is associated with oblate grains where the short axis is aligned in the direction of the current. This grain alignment will cause the resistivity of the medium to increase dramatically as the aspect ratio of the grains decreases.

Once the average geometric factor G has been determined, the mean free path length L again needs to be calculated. This is slightly different to the mean free path of a sphere because the axes of the ellipsoid have different lengths. The cross-sectional area (A_e) and the volume (V_e) of the ellipsoid are given by:

$$A_e = ab\pi\,, \tag{24}$$

$$V_e = 4\!\!\diagup\!\!_3\,\pi abc\,. \tag{25}$$

Equations 21–25 assume that the c-axis orientation is parallel to the direction of current flow. These equations can be worked through as was done in the case of the sphere (equations 11-15) to give the mean free path of ellipsoidal grains:

$$L = \frac{4c}{6(1-\beta)}\,. \tag{26}$$

The resistivity of the effective medium can then be determined in the same way as for spherical grains (equations 16-18). It can be seen that there is a marked change in the effective resistivity between the HS conductive bound and the geometric path length effective resistivity (Figure 7). The biggest change is seen when the oblate grains are oriented with their short axes aligned with the current. In this case the resistivity increases dramatically as porosity and aspect ratio decrease.

The above method calculates the maximum and minimum resistivity of an anisotropic medium. In order to calculate the resistivity when the current direction is neither parallel nor perpendicular to the long axis of the grains, we use an adapted version of Price's (1972) method. Price's method was originally used to determine the resistivity in any direction of an arbitrary-shaped sample of an anisotropic material; it was itself an extension of the van der Pauw (1958) method of measuring the resistivity of isotropic materials. For simplicity we will look at the two-dimensional problem in the x-y plane. In the isotropic case, when $\rho_x = \rho_y = \rho$, current density ($\underline{J}$) is given by:

$$\underline{J} = \frac{\underline{\underline{E}}}{\rho}, \tag{27}$$

where $\underline{E}$ is the electric field and is parallel to $\underline{J}$ and orthogonal to the electric equipotentials. However in the anisotropic case when $\rho_x \neq \rho_y$, $\underline{J}$ is now given as:

$$\underline{J} = \frac{E_x \underline{\hat{x}}}{\rho_x} + \frac{E_y \underline{\hat{y}}}{\rho_y}, \tag{28}$$

where E_x and E_y are components of the electric field in the x and y directions and $\underline{\hat{x}}$ and $\underline{\hat{y}}$ are unit vectors along the x and y axis respectively. The amplitude of J is then given by:

$$|\underline{J}| = \left[\frac{E_x^2}{\rho_x^2} + \frac{E_y^2}{\rho_y^2} \right]^{\frac{1}{2}} = \frac{\left[E_x^2 \rho_y^2 + E_y^2 \rho_x^2 \right]^{\frac{1}{2}}}{\rho_x \rho_y} . \qquad (29)$$

For a weakly anisotropic material (10% anisotropy as defined by the ratio of maximum to minimum resistivities) the relative current density amplitude changes almost sinusoidally with electric field angle and the change in amplitude is relatively small (Figure 8A). For a strongly anisotropic material (200% anisotropy) the change in amplitude is much greater and is also less sinusoidal (note different y-axis scales for 10% and 200% cases in Figure 8). Note that current density is deviated preferentially towards the direction of low resistivity in Figure 8A, and that the mean current density exceeds that which would be predicted by the arithmetic mean resistivity.

The azimuth angles of E (θ_E) and J (θ_J) can be given as:

$$\theta_E = \tan^{-1}\left(\frac{E_y}{E_x} \right), \qquad (30)$$

$$\theta_J = \tan^{-1}\left(\frac{J_y}{J_x} \right) = \tan^{-1}\left(\frac{E_y \rho_x}{E_x \rho_y} \right). \qquad (31)$$

Consequently the angle between the electric field direction and that of the current density is given by:

$$\delta\theta = \theta_E - \theta_J . \qquad (32)$$

For any anisotropic material J is no longer parallel to E, nor is it orthogonal to electric equipotentials when the electric field is not parallel to the minimum or maximum resistivity directions (Figure 8B). It also shows that as anisotropy increases the deviation angle increases. In a weakly anisotropic material the deviation angle varies

approximately sinusoidally with the electric field angle, but as the material becomes more anisotropic the relationship becomes more asymmetric.

Using the deviation angle and the current density we can now calculate the change in resistivity as the current (electric field) angle rotates around the anisotropic medium (Figure 8C). Again in the weakly anisotropic material the observed resistivity varies almost sinusoidally with electric current angle, whereas that of the strongly anisotropic material varies more asymmetrically. The mean resistivity, averaged over all directions of electric field across the sample, is lower than the average of the maximum and minimum resistivity.

By combining this result with the maximum and minimum resistivities calculated using the geometric path length method, we can now calculate the resistivity of the effective medium at any current angle and grain aspect ratio. Figure 9 shows an example of the change in resistivity of an effective medium composed of aligned oblate grains at a porosity of 30%.

Our two-phase effective medium method described above can be extended to three-phases in a similar way as Archie's Equation is often extended to three-phases. We can assume that the third phase is, for example, a hydrocarbon or hydrate, and that it has a high resistivity compared to the fluid. The porosity of the medium can be adjusted to accommodate the third phase, which effectively becomes part of the solid grain phase. The resistivity of the medium can then be calculated with this adjusted porosity using the geometric path length method. This approach assumes that the solid grains and the inclusions of the third phase material have the same aspect ratio.

COMPARISON WITH LABORATORY DATA

In Figure 4, we compared the predictions of our geometric path length (GPL) electrical effective medium model to those of the Hashin-Shtrikman conductive bound for the isotropic case. Ideally our model needs to be validated against physical observations on real two-phase systems. The most practical way to achieve this validation is to measure the electrical resistivity of sediment samples with known porosity and composition. Most real sediments are composed of many different types of grains each with their own physical properties and grain shape. Because our aim is to test a model in which the grains are treated as being made up of only a single material, we used artificial sediment cores composed of spherical glass beads with known physical properties, saturated with pore water of known composition and resistivity. The use of spherical grains results in isotropic sediments. We did not attempt to make anisotropic materials.

Method

The sediment specimens were prepared using a pluviation method. Pluviation provides reasonably homogeneous specimens (Rad and Tumay, 1985) and simulates the sediment fabric found in nature. It also produces the densest possible packing of mineral grains. The specimens were formed in a 50 cm plastic tube (of high electrical resistivity) with potential electrodes piercing the casing at 2 cm spacings. Spherical glass beads were used to simulate sediment grains. The pore fluid was composed of de-aired, distilled water which was made into brine by adding common salt (25g of

NaCl per 1 liter of water). Once filled with glass beads and brine, the sediment tube was sealed using pistons at each end incorporating current electrodes.

Electrical resistivity was measured by passing a current of 10 ± 0.01 mA through the end electrodes of the sediment specimen at a frequency of 220 Hz (Figure 10). These current electrodes were made from disks of stainless steel mesh in order to distribute the current as evenly as possible over the whole cross-section of the specimen and so minimize edge effects. The potential difference was measured between neighboring potential electrodes along the length of the core to an accuracy of ± 3.0 mV. Assuming that the current is distributed evenly through the cross-section of the sediment filled tube, resistivity was calculated to an accuracy of ± 3.6% using the equation:

$$\rho = \frac{VA}{DI} \tag{33}$$

where D is the distance between the potential electrodes, A is the cross-sectional area of the sediment cell (~32.5cm^2), V is the measured potential difference and I is the current.

Sediment density was measured at 0.5 cm intervals along the specimens using a multi-sensor sediment core logger (Gunn and Best, 1998). The density (gamma ray attenuation method) measurements are accurate to ± 0.07 g/cm^3. Sediment porosity was derived from the measured bulk densities using the relationship:

$$\varphi = \frac{\chi_s - \chi}{\chi_s - \chi_f}, \tag{34}$$

where χ is the sediment density, χ_s is the mineral density (2.50 ± 0.05 g/cm^3 for the glass beads), and χ_f is the brine density (1.02 ± 0.01 g/cm^3). The final porosity of the

samples ranged from 30% to 47% (± 3.4%). The resistivity of the pore fluid used in the laboratory samples was 0.36 ±0.01 Ωm. A total of 77 independent measurements were made on a set of 4 artificial sediment cores of varying porosity (Ellis, 2008).

Results

Figure 11 shows the comparison between the laboratory data and the predictions of Archie's equation (with various *m* and *a* coefficients), the HS conductive bound and the geometric path-length effective resistivity model developed in this paper. The *m* and *a* coefficients used to calculate the first Archie curve are both equal to 1.0, values that are generally used when modeling straight cylindrical pore channels (Herrick and Kennedy, 1994). The second Archie curve is calculated using *m* and *a* coefficients of 1.25 and 1 respectively; these values are generally used to calculate the resistivity of unconsolidated sands and spherical glass beads (Archie, 1942; Wyllie and Spangler, 1952; Atkins et al., 1961; Jackson et al., 1978). The third and fourth Archie curves were created using *m* and *a* coefficients recommended in the Schlumberger log interpretation charts for soft sediments (Schlumberger, 1977).

Although the laboratory measurements cover only a relatively narrow range of porosities, this is not necessarily a great disadvantage. Any satisfactory model will predict resistivities that converge to the solid phase resistivity at 0% porosity and to the liquid phase resistivity at 100% porosity, apart from Archie's equation when a is not equal to one. The largest deviations between model predictions are likely to occur at mid-range porosities where our experimental data are located. Also the range of porosities covered by our laboratory measurements is similar to that encountered in many natural sedimentary formations of interest.

An RMS misfit was calculated between the predictions of each of the models and the laboratory data (Table 1). Both the HS conductive bound and the Geometric path-length effective resistivity models predict the resistivities reasonably well. However, three of the four Archie curves do not go through any of the resistivity data points. The geometric path-length effective resistivity model has the lowest RMS misfit to the laboratory data, improving on both the HS conductive bound and the second Archie equation curve ($m = 1.25$, $a = 1$).

Although the geometric path-length effective resistivity model does fit the data better than the other models overall, it does not fit all the data points within the experimental errors. There may be several reasons for this. Firstly, four separate sediment specimens were made in the laboratory. While every endeavor was made to ensure they were identical in terms of composition, there may have been small differences in the pore fluid salinity and impurities in the sediment grains. This could have affected the final resistivity of the sediment, factors outside the scope of the model. It was also assumed that the temperatures at which the sediments were measured were the same for all specimens. In fact, small changes in temperature can cause large differences in the measured resistivity. Finally, the porosity measurements are averages over the whole cross-section of the sediment tube even though porosity may vary locally and hence deviate from the single value used to model each specimen.

CONCLUSION

We have developed a physical effective medium model for predicting the electrical resistivity of two-phase geological materials. The model assumes that the fluid phase is fully interconnected and is the less resistive constituent. The

geometrical arrangement of the solid inclusions is specified in terms of overall porosity and the aspect ratio of ellipsoidal grains. The method allows both the fluid and solid phases to possess some conductivity, which is important for modeling sediments with clay minerals (electric double layers) and other surface charge effects at high salinities. The method uses a geometric factor and mean path length approach to take account of the increase in path length taken by mobile charge carriers which are distributed preferentially in the fluid phase. The resistivity is dependent on the porosity and the aspect ratio of the grains, but is independent of grain size. Therefore it can be applied to a wide range of sedimentary formations.

The two-phase geometric path-length effective resistivity model was found to predict the observed resistivities in synthetic sediment specimens. It produced a better fit than either the HS conductive bound, or Archie's equation with the m and a coefficients commonly used for soft formations or for loose glass bead samples.

The isotropic two-phase model was extended to the case of electrical anisotropy by aligning ellipsoidal grains with an aspect ratio of less than one. However, experimental data of electrical anisotropy in sediments and sedimentary rocks are needed to verify the anisotropic model predictions. Under a limited set of conditions, the geometric path-length effective resistivity model can also be extended to include a third, resistive, phase. This could be applied to the prediction of water saturation from resistivity measurements on, for example, partially gas saturated, or gas hydrate-bearing, sediments. Again, more experimental data are needed to verify the model predictions.

ACKNOWLEDGEMENTS

Michelle Ellis was supported by an Ocean Margins LINK PhD studentship from the United Kingdom Natural Environment Research Council.

REFERENCES

Anderson, B., and K. Helbig, 1994, Oilfield Anisotropy: Its origins and Electrical Characteristics: Oilfield Review, **6**, no. 4, 48-56.

Archie, G. E., 1942, The electrical resistivity log as an aid in determining some reservoir characteristics: Transactions of the American Institute of Mining Engineers, **146**, 54-62.

Atkins, E. R., and G. H. Smith, 1961, The significance of particle shape in formation factor porosity relationships: Journal of Petroleum Technology, **13**, 285-291.

Berg, C. R., 1995, A simple, effective-medium model for water saturation in porous rocks: Geophysics, **60**, 1070-1080.

Bruggeman, D. A.G., 1935, Berechnung verschiedener physikalischer konstanten von heterogenen Substanzen: Ann. Physik, **24**, 636-664.

Bussian, A. E., 1983, Electrical conductance is a porous medium: Geophysics, **48**, 1258-1268.

Clavaud, J. B., 2008, Intrinsic electrical anisotropy of shale: the effect of compaction: Petrophysics, 49, 243-260,

Clavier, C., G. Coates, and J. Dumanoir, 1984. Theoretical and experimental bases for the dual-water model for interpretation of shaly sands: Society of Petroleum Engineers Journal, **4**, 153–168.

Ellis, M. H., 2008, Joint seismic and electrical measurements of gas hydrates in continental margin sediments: PhD. thesis, University of Southampton.

Gunn, D. E., and A. I. Best, 1998, A new automated non-destructive system for high resolution multi-sensor core logging of open sediment cores: Geo-marine Letters, **18**, 70-77.

Hanai, T., 1960, Theory of the dielectric dispersion due to the interfacial polarization and its application to emulsion: Kolloid Z, **171**, 23–31.

Hashin, Z., and S. Shtrikman, 1962, A variational approach to the theory of the effective magnetic permeability of multiphase materials: Journal of Applied. Physics, **33**, 3125–3131.

Herrick, D. C., and W. D. Kennedy, 1994, Electrical efficiency: a pore geometric-theory for interpreting the electrical properties of reservoir rocks: Geophysics, **59**, 918 -927.

Jackson, P. D., D. Tayor-Smith, and P. N. Stanford, 1978, Resistivity-porosity-particle shape relationships for marine sands: Geophysics, **43**, 1250-1268.

Mavko, G., T. Mukerji, and J. Dvorkin, 1998, The Rock Physics Handbook: Tools for Seismic Analysis in Porous Media: Cambridge University Press.

Price, W. L. V., 1972. Extension of van der Pauw's theorem for measuring specific resistivity in discs of arbitrary shape to anisotropic media: Journal of Physics D: Applied Physics, **5**, 1127-1132.

Rad, N. S., and M. T. Tumay, 1985, Factors Affecting Sands Specimen Preparation by Raining: Geotechnical Testing Journal, **10,** 31-37.

Schlumberger, 1977, Log Interpretation Charts, Schlumberger Limited.

Sen, P. N., Scala, C., and Cohen, M. H., 1981, A self-similar model for sedimentary rocks with application to the dielectric constant of fused glass beads: Geophysics, 46, 781-795.

Van der Pauw, L. J., 1958, A method of measuring specific resistivity and Hall effect of discs of arbitrary shape: Philips Research Reports, **13**, 1-9.

Waxman, M. H., and L. J. M. Smits, 1968, Electrical conductivities in oil-bearing shaly sand: Society of Petroleum Engineers Journal, **8**, 107-122.

Wyllie, M. R. J., and P. F. Southwick, 1954, An experimental investigation of the S. P. and resistivity phenomena in dirty sands: Journal of Petroleum Technology, **6**, 44-57.

Wyllie, M. R. J., and M. B. Spangler, 1952, Application of electrical resistivity measurements to the problem of fluid flow in porous media: Bulletin of the American Association of Petroleum Geology, **36**, 359-403.

FIGURES CAPTIONS

Figure 1: The deviation of electric current around a spherical grain.

Figure 2: Calculation of the path length (geometric factor in equations 4 – 9) for electric current traveling in the z direction when encountering a spherical grain: (A) in a plane through the z-axis and (B) in the x-y plane.

Figure 3: The relationship between the mean free path length (L), the average un-deviated path length (l_{2ave}) and the radius of the grain (r).

Figure 4: Comparison of the HS conductive bound model, the geometric resistivity model and the geometric path length effective resistivity for a range of porosities. The fluid has a resistivity of 0.36 Ωm and the solid has a resistivity of 300 GΩm.

Figure 5: Relative lengths of the semi-axes of oblate and prolate grains when the grains are in their most and least resistive orientations. Current direction is always parallel to the c semi-axis.

Figure 6: Geometric factor as a function of grain aspect ratio for fully aligned oblate and prolate grains in the most and least resistive alignments.

Figure 7: Resistivity (Ωm) for oblate grains calculated using the HS conductive bound model (top), and the geometric path length effective resistivity method where the grains are aligned in the most resistive direction (middle) and the least resistive direction (bottom). Grain and fluid resistivities are as in Figure 4.

Figure 8: Current density (A), deviation angle between current density and electric field (B), and resistivity (C) as a function of electric field angle. Black lines indicate the values for a weakly anisotropic material where ρ_{min} = 1 Ωm and

ρ_{max} = 1.1 Ωm (10% anisotropy). Grey lines indicate values for a strongly anisotropic material where ρ_{min} = 1 Ωm and ρ_{max} = 3 Ωm (200% anisotropy). In each plot, the y-axis scale for the weakly anisotropic material is given on the left and the strongly anisotropic material on the right.

Figure 9: Anisotropic geometric path-length effective resistivity model model resistivity results as a function of electric field angle for selected oblate grain aspect ratios. Porosity is 30%, grain and fluid resistivities are as in Figure 4.

Figure 10: Experimental setup for laboratory measurements of resistivity on artificial sediment samples.

Figure 11: Comparison of artificial sediment experimental data (4 different specimens, frequency = 220 Hz, temperature = 6 °C,) with model predictions from Archie's equation with different cementation and the tortuosity constants, from the HS conductive bound model, and from the geometric path-length effective resistivity model.

TABLE CAPTIONS

Table 1: Root-mean-square (RMS) misfit values between the electrical model predictions (Archie, HS and geometric path-length effective resistivity model models) and the laboratory resistivity measurements on artificial sediments in Figure 11.

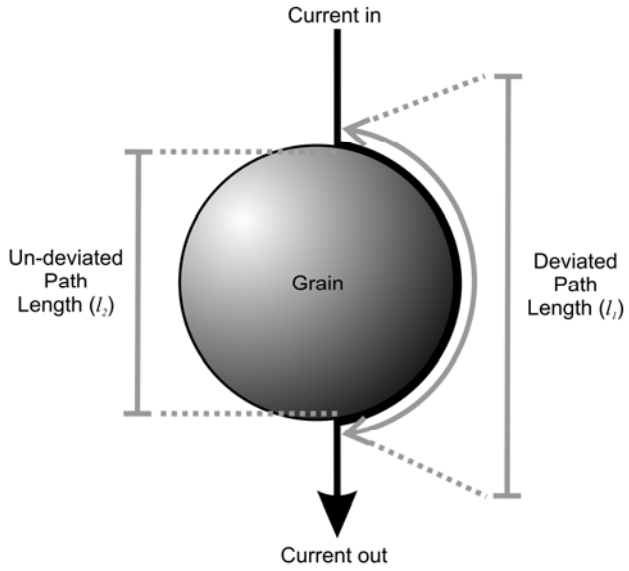
Current in
Un-deviated
Path
Length (l_2)
Grain
Deviated
Path
Length (l_1)
Current out

Fig 1

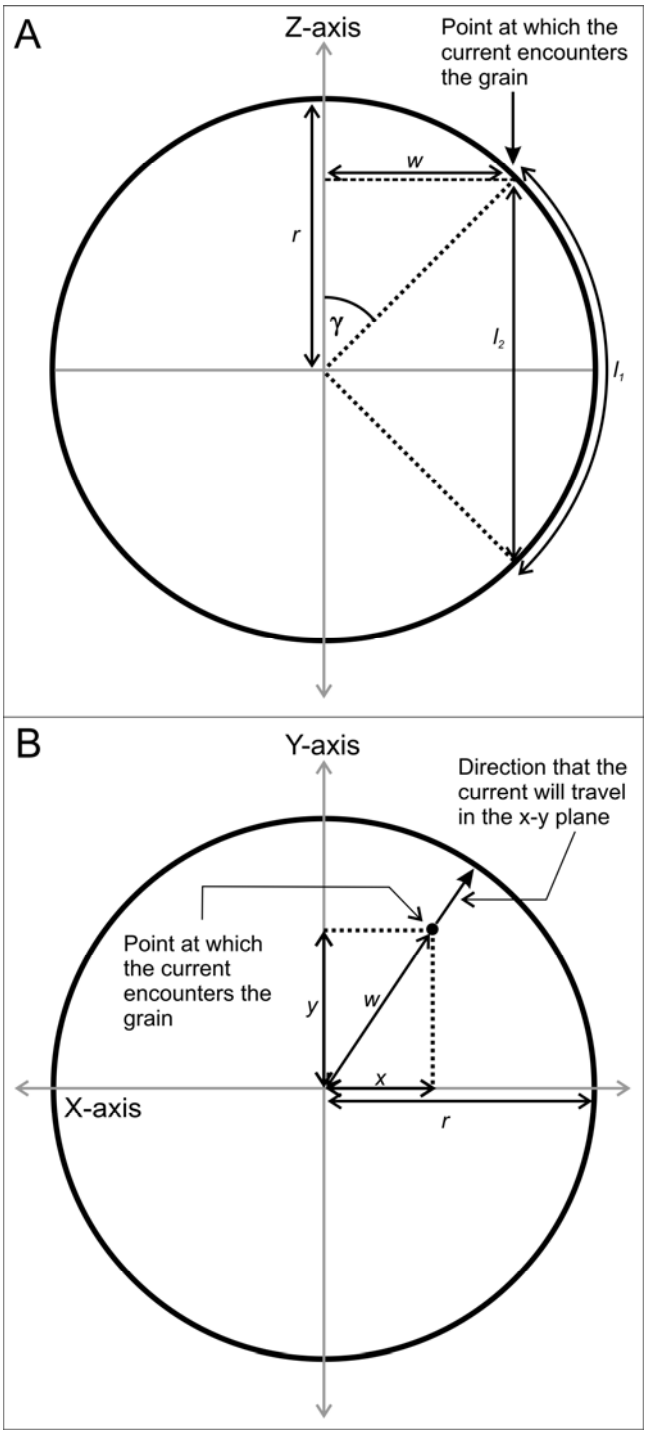
A
Z-axis
Point at which the current encounters the grain
w
r
γ
l_2
l_1
B
Y-axis
Direction that the current will travel in the x-y plane
Point at which the current encounters the grain
y
w
x
X-axis
r

Fig 2

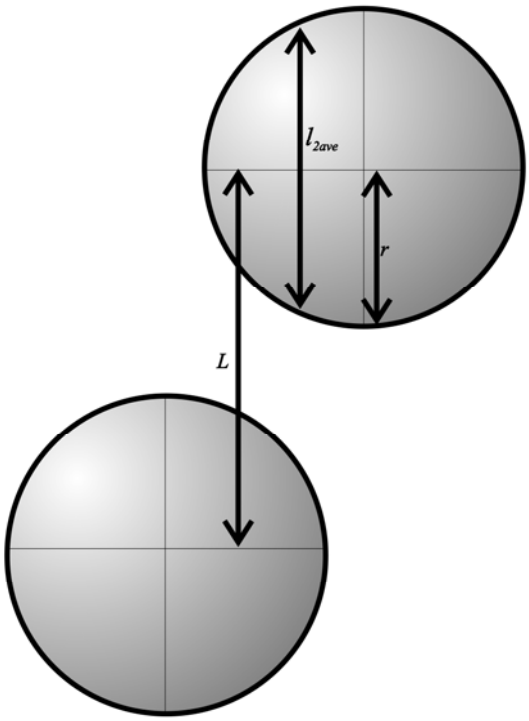

Fig 3

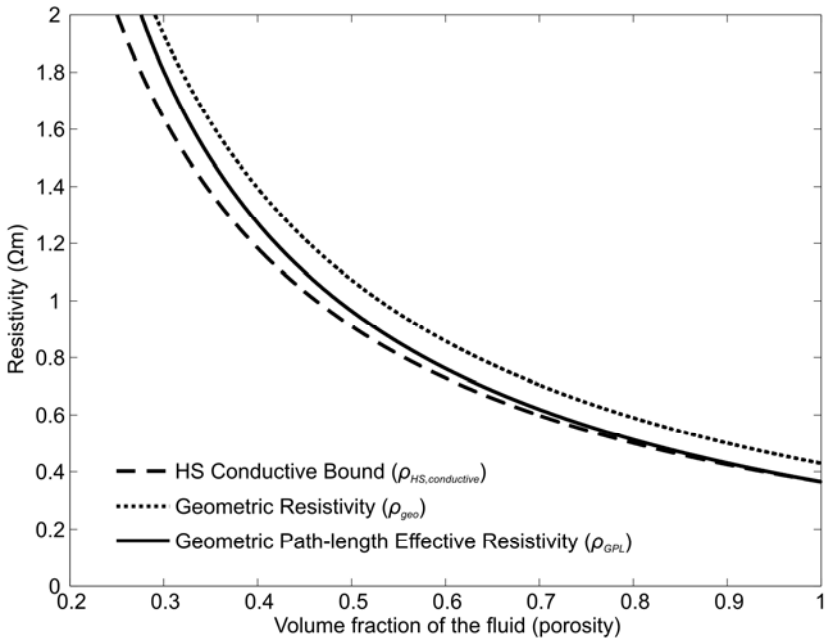
Resistivity (Ωm)
Volume fraction of the fluid (porosity)
HS Conductive Bound ($\rho_{HS,conductive}$)
Geometric Resistivity (ρ_{geo})
Geometric Path-length Effective Resistivity (ρ_{GPL})
0
0.2
0.4
0.6
0.8
1
1.2
1.4
1.6
1.8
2
0.2
0.3
0.4
0.5
0.6
0.7
0.8
0.9
1

Fig 4

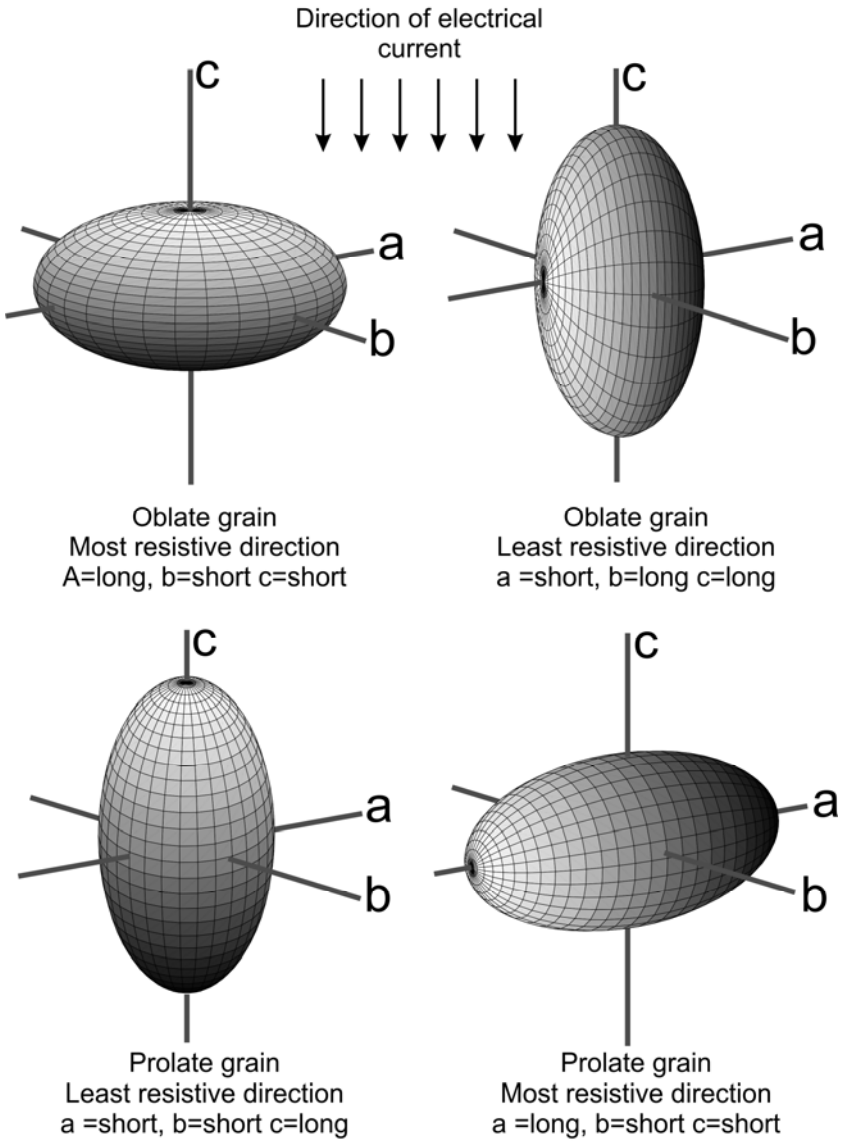
Direction of electrical current
c
a
b
Oblate grain
Most resistive direction
A=long, b=short c=short
c
a
b
Oblate grain
Least resistive direction
a =short, b=long c=long
c
a
b
Prolate grain
Least resistive direction
a =short, b=short c=long
c
a
b
Prolate grain
Most resistive direction
a =long, b=short c=short

Fig 5

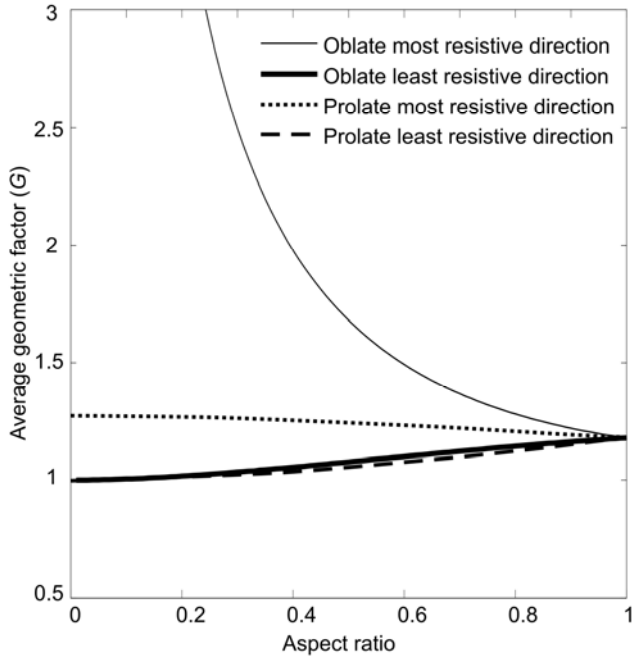
Oblate most resistive direction
Oblate least resistive direction
Prolate most resistive direction
Prolate least resistive direction
Average geometric factor (G)
Aspect ratio
3
2.5
2
1.5
1
0.5
0
0.2
0.4
0.6
0.8
1

Fig 6

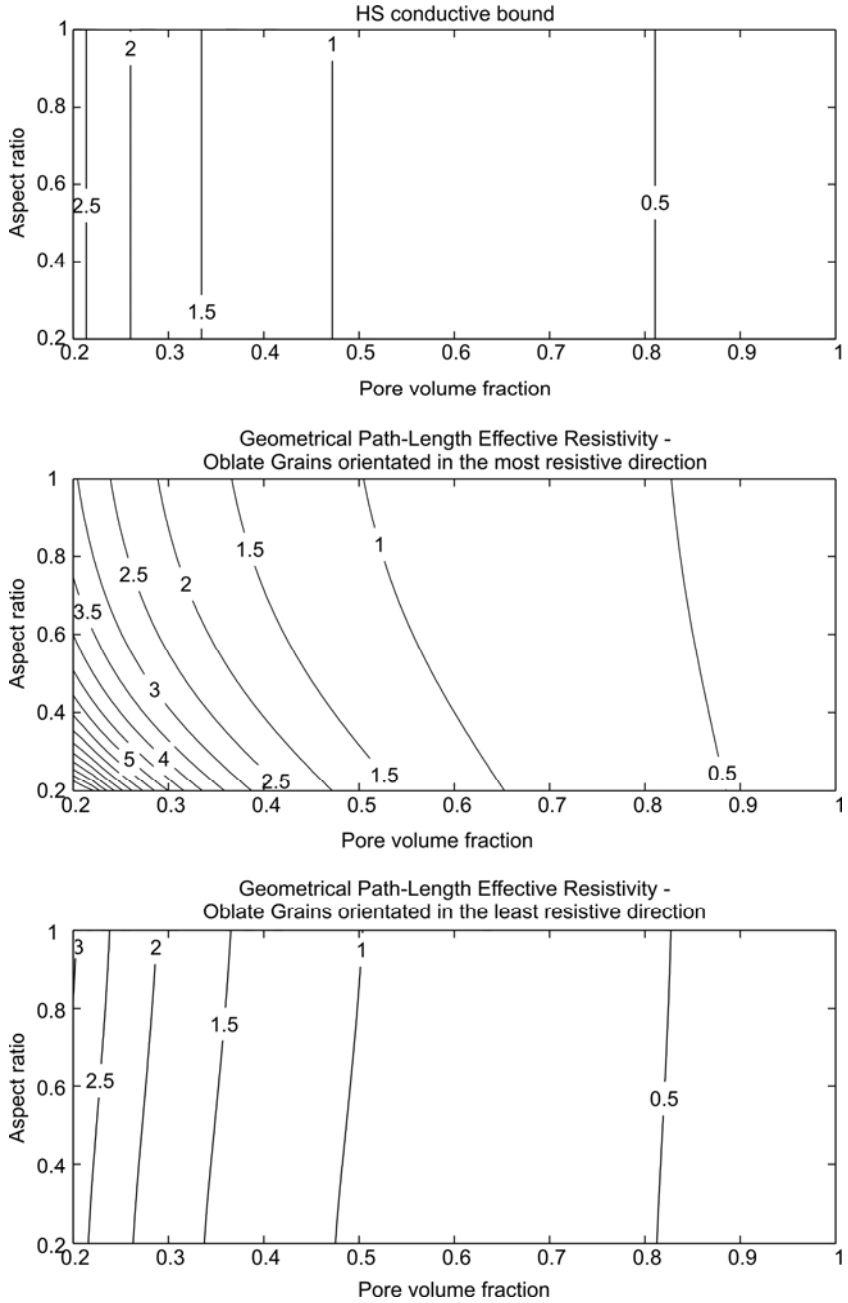
HS conductive bound
Aspect ratio
Pore volume fraction
2
1
2.5
0.5
1.5
Geometrical Path-Length Effective Resistivity -
Oblate Grains orientated in the most resistive direction
Aspect ratio
Pore volume fraction
1.5
1
2.5
2
3.5
3
5
4
2.5
1.5
0.5
Geometrical Path-Length Effective Resistivity -
Oblate Grains orientated in the least resistive direction
Aspect ratio
Pore volume fraction
3
2
1
1.5
2.5
0.5

Fig 7

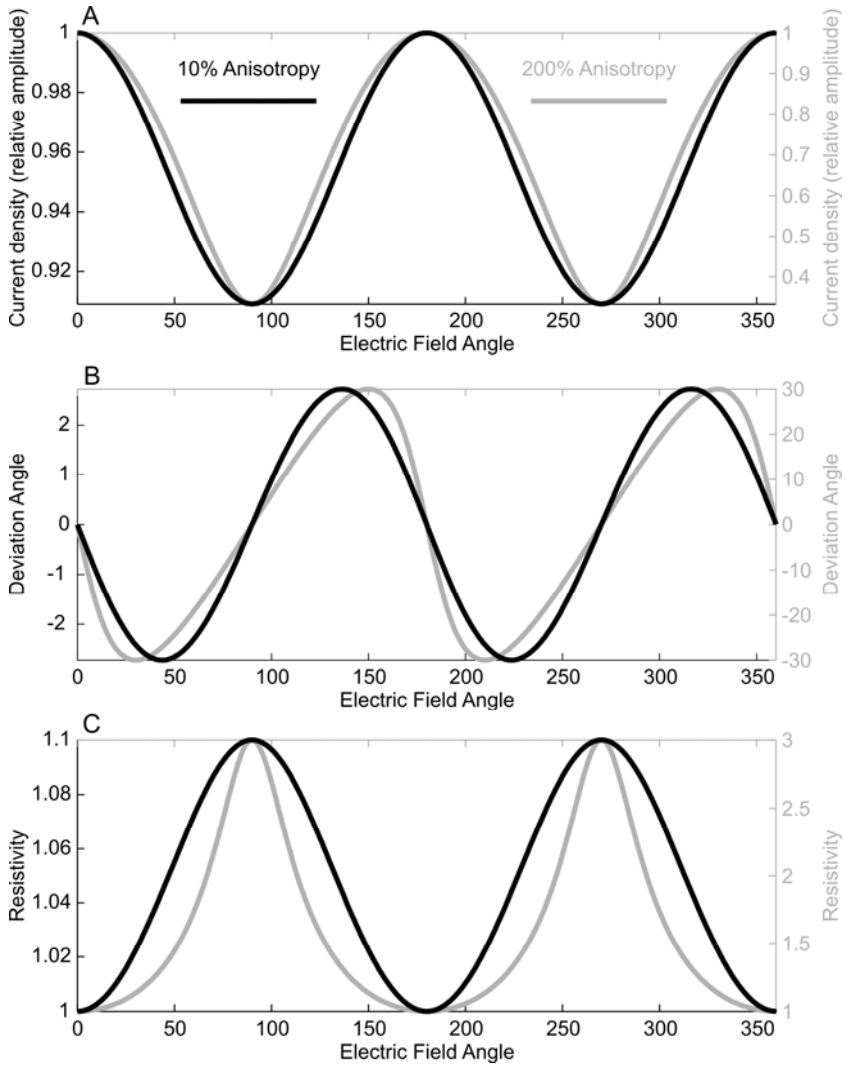
A
10% Anisotropy
200% Anisotropy
Current density (relative amplitude)
Electric Field Angle
B
Deviation Angle
Electric Field Angle
C
Resistivity
Electric Field Angle

Fig 8

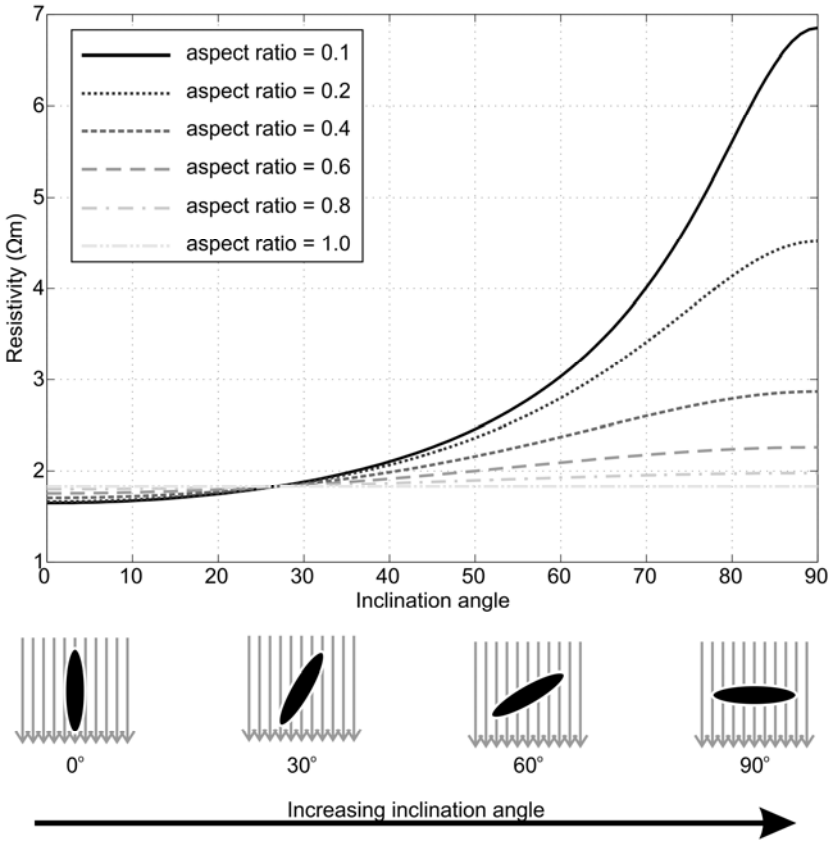
aspect ratio = 0.1
aspect ratio = 0.2
aspect ratio = 0.4
aspect ratio = 0.6
aspect ratio = 0.8
aspect ratio = 1.0
Resistivity (Ωm)
Inclination angle
0°
30°
60°
90°
Increasing inclination angle

Fig 9

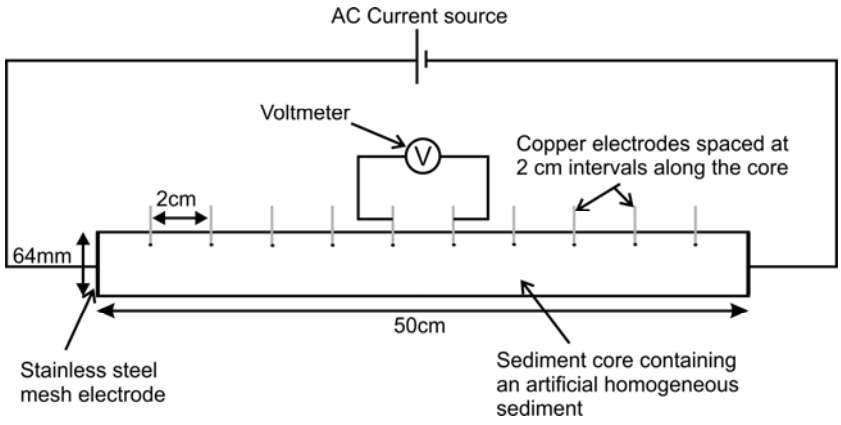
AC Current source
Voltmeter
V
Copper electrodes spaced at
2 cm intervals along the core
2cm
64mm
50cm
Stainless steel
mesh electrode
Sediment core containing
an artificial homogeneous
sediment

Fig 10

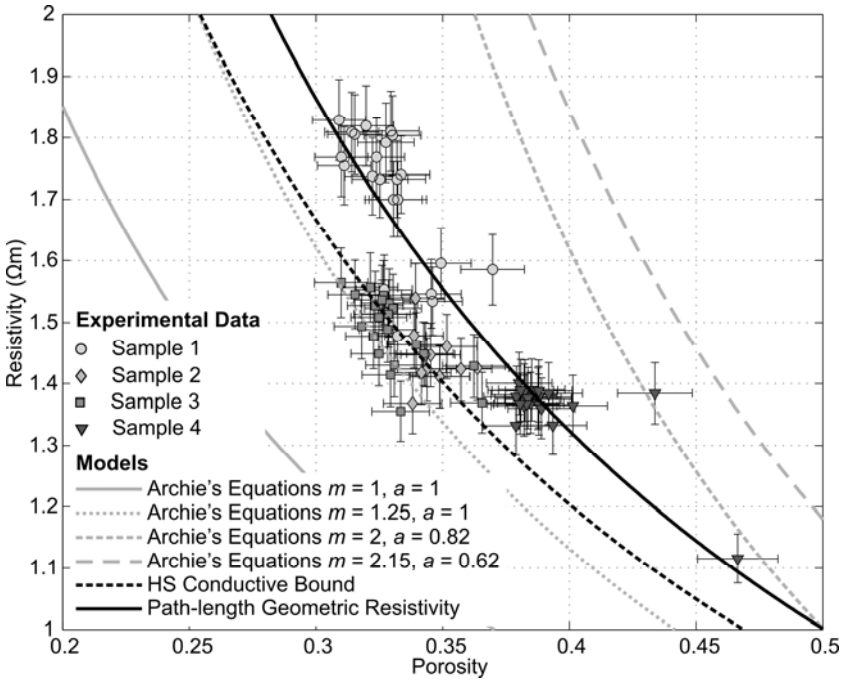
Resistivity (Ωm)
Porosity
2
1.9
1.8
1.7
1.6
1.5
1.4
1.3
1.2
1.1
1
0.2
0.25
0.3
0.35
0.4
0.45
0.5
Experimental Data
Sample 1
Sample 2
Sample 3
Sample 4
Models
Archie's Equations m = 1, a = 1
Archie's Equations m = 1.25, a = 1
Archie's Equations m = 2, a = 0.82
Archie's Equations m = 2.15, a = 0.62
HS Conductive Bound
Path-length Geometric Resistivity

Fig 11

Model	Resistivity RMS misfit (Ωm)
Archie's equation (where $m = 1$, $a = 1$)	0.451
Archie's equation (where $m = 1.25$, $a = 1$)	0.183
Archie's equation (where $m = 2.15$, $a = 0.62$)	0.765
Archie's equation (where $m = 2$, $a = 0.81$)	1.007
HS conductive bound	0.134
Geometric Path-length Effective Resistivity	0.123

Table 1